

(A4a). Before carrying out the expansion we will put $\psi_{s(\text{sc})}^+$ in a more convenient form by using the operator identity

$$Q_j[E+i\eta-K]^{-1}T=[E+i\eta-K_{j'}]^{-1}T_{j'}Q_j, \quad (\text{A5a})$$

where j' is arbitrary, and

$$T_{j'}=V_j+V_{j'}[E+i\eta-H]^{-1}V_j, \quad (\text{A5b})$$

$$V_j=Q_jVQ_j, \quad (\text{A5c})$$

$$K_j=H-V_j. \quad (\text{A5d})$$

This leads to the expression

$$\begin{aligned} \langle \chi_{s(a)} | \psi_{s(\text{sc})}^+ \rangle &= \frac{(Z+1)^{-1}}{E+i\eta-E_a} \sum_{kj} \delta_k \delta_j \langle Q_k \chi_a | T_{kj} | Q_j \chi \rangle \\ &= [E+i\eta-E_a]^{-1} \\ &\quad \times \{ T_a(\mathbf{p}_a, \mathbf{p}) - Z T_a^{\text{ex}}(\mathbf{p}_a, \mathbf{p}) \}, \quad (\text{A6a}) \end{aligned}$$

where

$$T_a(\mathbf{p}_a, \mathbf{p}) = \langle \chi_a | T | \chi \rangle, \quad (\text{A6b})$$

$$T_a^{\text{ex}}(\mathbf{p}_a, \mathbf{p}) = \langle \chi_a | T_{0k} | \chi \rangle, \quad (\text{A6c})$$

with $k \neq 0$. $\Psi_{s(\text{sc})}(t)$ is thus

$$\begin{aligned} \Psi_{s(\text{sc})}(t) &= (Z+1)^{1/2} \\ &\quad \times \mathcal{S} \sum_a \frac{\chi_a}{E+i\eta-E_a} \{ T_a(\mathbf{p}_a, \mathbf{p}) - Z T_a^{\text{ex}}(\mathbf{p}_a, \mathbf{p}) \}. \quad (\text{A7}) \end{aligned}$$

Following the same line of development as in Sec. II, this may be put in the form

$$\Psi_{s(\text{sc})}(t) = (Z+1)^{1/2} \mathcal{S} \Psi_{\text{sc}}(t), \quad (\text{A8})$$

where $\Psi_{\text{sc}}(t)$ is given by Eq. (9) with f_a defined by (10). The decay process is now described by

$$\Psi_{s(\text{dc})}(t) = (Z+1)^{1/2} \mathcal{S} \Psi_{\text{dc}}(t) \quad (\text{A9})$$

which is obtained from (A8) by replacing h with H_r and including the initial state of the radiation field. In the same way that one verifies (A4a), it is readily verified that

$$\begin{aligned} \langle P(t) \rangle &\equiv \langle \Psi_{s(\text{dc})}(t) | P | \Psi_{s(\text{dc})}(t) \rangle \\ &= \langle \Psi_{\text{dc}}(t) | P | \Psi_{\text{dc}}(t) \rangle. \quad (\text{A10}) \end{aligned}$$

Thus the symmetrization in (A9) may be ignored for the purpose of calculating the photon counting rate.

Superconducting Transitions of Amorphous Bismuth Alloys*†

J. S. SHIER‡ AND D. M. GINSBERG§

Department of Physics and Materials Research Laboratory, University of Illinois, Urbana, Illinois

(Received 20 December 1965)

Measurements have been made of the critical temperatures T_c of binary-alloy films composed of amorphous bismuth with lead, thallium, or antimony in concentrations up to 13 at.%. The curves showing T_c as a function of impurity concentration are nearly linear, as expected for a superconductor with no crystalline anisotropy. The slopes of the curves are not simply related to the valence or free-atom size of the impurity atoms. It is suggested that this may be explainable by extending Faber and Ziman's theory of the breakdown of Linde's rule for liquid alloys. The transitions of the films into the superconducting state are extremely sharp (~ 5 mdeg wide). This indicates strongly that the electromagnetic coherence length does not limit the sharpness of the transition.

I. INTRODUCTION

THE superconducting critical temperatures of many different alloys have been measured in the last 50 years. However, only in the last few years have we had the theoretical knowledge required to examine the fundamental significance of the data. All of our present theoretical understanding of critical temperatures has,

of course, arisen from the BCS theory,¹ and from elaborations on it. Two years after this theory was presented, Anderson made a major advance by suggesting two mechanisms which usually dominate the shift in the critical temperature T_c of a metal as impurities are added.² He suggested that nonmagnetic impurities depress T_c because of a decrease in the effect of crystal anisotropy on the electrons. This is called the anisotropy effect. He also showed that magnetic impurities are expected to cause an additional depression of T_c , because of their tendency to break down the electron pair-

* This research was supported in part by the Advanced Research Projects Agency under Contract No. SD-131 and in part by the National Science Foundation.

† Based on the Ph.D. thesis of J. Shier, University of Illinois, 1966 (unpublished).

‡ Present address: Los Alamos Scientific Laboratory, Los Alamos, New Mexico.

§ A. P. Sloan Fellow during part of this research.

¹ J. Bardeen, L. N. Cooper, and J. R. Schrieffer, Phys. Rev. **108**, 1175 (1957).

² P. W. Anderson, J. Phys. Chem. Solids **11**, 26 (1959).

ing in the superconducting state. In this paper, we will confine our discussion to nonmagnetic impurities. For these, Anderson pointed out that the reduction in T_c should be sharpest as the impurities reduce the electron mean free path to about the size of the coherence length ξ_0 in the pure metal. The anisotropy effect is therefore expected to be a nonlinear function of impurity concentration.

A number of theoretical calculations have been carried out on the basis of these ideas.³⁻⁷ The calculation of Markowitz and Kadanoff,⁵ which has had experimental support,⁸ provides results which can be compared rather directly with experimental data. These authors fitted parameters in their theory to the extensive and systematic experimental data which were available for binary alloys consisting mostly of tin, indium, or aluminum. The contribution to the shift in T_c arising from influences other than the anisotropy effect is called the valence effect.⁵ The fitting of the theoretical parameters to the data relies on the assumption that the valence effect is proportional to impurity concentration, so it can be separated from the anisotropy effect, which is a nonlinear function of impurity concentration.⁹

In this paper, we will define δT_c as the shift in T_c caused by the valence effect. For alloys of tin, indium, and aluminum, δT_c is known, because Markowitz and Kadanoff have theoretically found the anisotropy effect, which can then be subtracted from the observed shifts in critical temperature to yield δT_c . If small amounts of impurities are added to a metal, the conduction-electron concentration and reciprocal mean free path are changed in direct proportion to the impurity concentration. (The reciprocal mean free path may become nonlinear in impurity concentration for large concentrations.¹⁰) Since the valence effect is believed to be linear in the impurity concentration, it is reasonable to assume that δT_c depends linearly on the conduction-electron concentration and the reciprocal mean free path. It has been shown¹¹ that, for the alloys considered by Markowitz and Kadanoff in which there is no precipitation, δT_c can be convincingly analyzed in this way so that

$$\delta T_c = \alpha \delta \rho + \beta n^i \delta z. \quad (1)$$

In this equation, $\delta \rho$ is the impurity-induced low-temperature normal-state resistivity divided by the increase in resistivity which appears when the metal is warmed up from 4 to 273°K. The quantity $\delta \rho$ should therefore be proportional to the impurity-induced change in reciprocal mean free path. The other symbols in Eq. (1) are defined as follows: n^i is the concentration of impurity atoms, δz is the difference between the number of conduction electrons per atom in the impurity and that of the host metal, and the constants α and β depend only on the host metal.

It has been shown how the term $\alpha \delta \rho$ can be calculated from the change in the electron-phonon coupling, if effects of crystal structure can be ignored.¹² Effects which might arise from the change in molar volume are expected to be negligible in the alloys considered, although they may be important for other alloys.¹³⁻¹⁶ Brillouin-zone effects have also been seen at times,^{8,17} although they are usually small. A sizeable shift in T_c can result from precipitation.¹⁸

We have measured the critical temperatures of a series of binary alloys in which the major constituent is amorphous bismuth. This is known to be superconducting,¹⁹ and to have no long-range lattice order.^{20,21} Therefore, there should be no anisotropy effect, Brillouin-zone effect, or precipitation. The valence effect δT_c can be observed directly, avoiding uncertainties introduced by using a theoretical analysis to subtract the anisotropy effect from the observed shifts in critical temperature. In this way, we can find out whether δT_c is proportional to the impurity concentration in dilute alloys, as theorists have assumed, and whether δT_c can be expressed in the form given by Eq. (1). There have been some previous studies of the transition temperatures of amorphous bismuth alloys,^{22,23} but they are not suitable for testing the validity of Eq. (1), because only a few widely spaced compositions were investigated. The data also yield information about the coherence lengths in the superconducting samples, which we will discuss later.

II. EXPERIMENTAL METHODS

A. General Description

The amorphous bismuth alloy films are produced in a metal cryostat by evaporating the alloys from a hot tungsten filament onto a cold substrate. To ensure

³ T. Tsuneto, Progr. Theoret. Phys. (Kyoto) **28**, 857 (1962).
⁴ C. Caroli, P. G. de Gennes, and J. Matricon, in *Metallic Solid Solutions*, edited by J. Friedel and A. Guinier (W. A. Benjamin, Inc., New York, 1963), Vol. XXIII.
⁵ D. Markowitz and L. P. Kadanoff, Phys. Rev. **131**, 563 (1963).
⁶ P. Hohenberg, Zh. Eksperim. i Teor. Fiz. **45**, 1208 (1963) [English transl.: Soviet Phys.—JETP **18**, 834 (1964)].
⁷ D. M. Brink and M. J. Zuckerman, Proc. Phys. Soc. (London) **85**, 329 (1965).
⁸ D. Farrell, J. G. Park, and B. R. Coles, Phys. Rev. Letters **13**, 328 (1964); **13**, 650 (E) (1964).
⁹ It is important to note that the anisotropy effect is thought to continue to shift T_c , even at large impurity concentrations; the effect does not saturate (see Ref. 5).
¹⁰ J. M. Ziman, *Electrons and Phonons* (Oxford University Press, New York, 1960), Chap. IX.
¹¹ D. M. Ginsberg, Phys. Rev. **136**, A1167 (1964).

¹² D. M. Ginsberg, Phys. Rev. **138**, A1409 (1965).
¹³ W. DeSorbo, Phys. Rev. **140**, A914 (1965).
¹⁴ R. I. Gayley, Phys. Letters **13**, 278 (1964).
¹⁵ L. T. Claiborne, J. Phys. Chem. Solids **24**, 1363 (1963).
¹⁶ L. T. Claiborne, J. Phys. Chem. Solids **26**, 653 (1965).
¹⁷ M. F. Merriam, Rev. Mod. Phys. **36**, 152 (1964).
¹⁸ R. E. Mould and D. E. Mapother, Phys. Rev. **125**, 33 (1962).
¹⁹ W. Buckel and R. Hilsch, Z. Physik **138**, 109 (1954).
²⁰ W. Buckel, Z. Physik **138**, 136 (1954).
²¹ W. Buckel, in *Structure and Properties of Thin Films*, edited by C. A. Neugebauer, J. B. Newkirk, and D. A. Vermilyea (John Wiley & Sons, Inc., New York, 1959), p. 53.
²² N. Barth, Z. Physik **142**, 58 (1955).
²³ W. Buckel and R. Hilsch, Z. Physik **146**, 27 (1956).

homogeneity, we have chosen alloying impurities with vapor pressures which are not too different from that of bismuth, so their rates of evaporation from the tungsten filament are about the same as that of bismuth. Homogeneity is further promoted by flash-evaporating small alloy pellets from the filament, building up the sample in layers, each about 80 Å thick. At the same time the sample is made, a "dummy" sample with a larger area is made on an identical substrate, held at the same temperature. The dummy sample can be chemically analyzed. The critical temperature of the sample film is found by measuring its electrical resistivity as a function of temperature. The sample is maintained in a vacuum at low temperature throughout the measurements, since it would become crystalline if it were allowed to warm up above a certain temperature, which is about 20°K for pure bismuth films a few hundred Å thick.^{22,23} After our determination of a film's critical temperature, and before the film is exposed to air, a silver film is evaporated over it. The thickness of the resulting step at the edge of the sample film is then measured by multiple beam interferometry to determine the thickness of the film.²⁴ This measurement is made at room temperature. Although the density of the film decreases slightly when it crystallizes while warming to room temperature, the thickness of the crystallized film should be proportional to the thickness of the amorphous film, and this provides us with all the information we need.

B. Cryogenics

A schematic drawing of the cryostat is shown in Fig. 1. The substrate is mounted on a copper block, which is attached by Wood's metal to a small (0.5-l) liquid-helium tank. The copper block has recessed areas where two substrates are placed, one for the sample and one for the "dummy" sample. They are surrounded by two

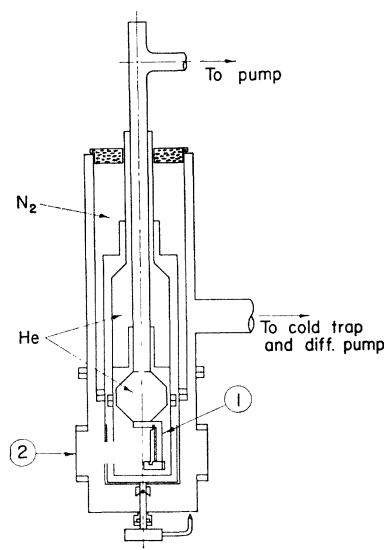


FIG. 1. Schematic cross section through the cryostat. (1) Copper substrate holder; (2) side port for mounting vapor sources.

²⁴ B. J. Stern, *Rev. Sci. Instr.* **34**, 152 (1963).

heat shields, one at 4.2°K and the other at 77°K. A shutter inside the 77°K shield allows a hole to be opened, so a film can be deposited from a hot filament located outside the cold region.

A heater consisting of numerous turns of manganin wire is wound on a copper drum and potted with GE 7031 cement, with an epoxy layer over it to reduce out-gassing. The heater is mounted at the top of the copper block by two screws passing through holes in mounting lugs on the copper drum. Indium gaskets are tightly compressed between the lugs and the copper block to provide good thermal contact. A copper holder for a calibrated germanium resistance thermometer is fastened to the back of the copper block behind the sample in the same way. This thermometer is placed in a $\frac{1}{8}$ -in.-diam hole in the holder, with thermal contact provided by Apiezon T grease.

A mask holder, running in two grooves, travels horizontally in front of the substrates. It holds four masks, used to outline the area of vapor deposition on both the sample and dummy substrates, in either of two positions. Changing of the masks is accomplished by a pinion gear, which engages teeth on the bottom of the mask holder. The end of the pinion gear shaft is slotted to engage a screwdriver blade on a retractable shaft, which can be inserted through holes in the heat shields. The mask holder is connected by a section of stranded copper wire to the copper block, to ensure thermal equilibrium.

The electrical wires leading to the sample area are thermally anchored to each of the heat shields, and to the small helium tank. Both heat shields have holes to allow the metal vapor to fall on the substrate, and to allow the retractable shaft to be inserted. The outer heat shield has a rotary copper shutter, which is used to block these holes during the critical temperature measurements. This shutter is connected to the shield by a heavy copper braid. The shutter is operated by a retractable thin-walled inconel tube, which passes into the vacuum space through an O-ring seal at the bottom of the cryostat. The small helium tank, to which the substrate holder is attached, is provided with a pumping tube leading out through the top of the cryostat, so that the temperature of the substrate can be lowered to 1.1°K. At the bottom, the outside of the cryostat consists of a demountable brass bell jar, sealed by a neoprene O-ring. The bell jar has four side ports, which are used to mount the evaporator filament, a viewing window, and the retractable shaft assembly used to operate the mask changer inside the heat shields.

C. Film Preparation

The substrates are *z*-cut plates of single-crystal quartz, with dimensions $\frac{1}{2} \times 1 \times \frac{1}{32}$ in. The single-crystal substrate provides good thermal contact between the surface where the film is deposited and the copper block in contact with the helium bath. (Use of a glass sub-

strate may possibly account for the rather broad transition observed by Zavaritskii in amorphous bismuth.²⁵) Thermal contact between the quartz plate and the copper block is provided by a thin layer of gallium. (Liquid gallium wets quartz well, and will wet copper if it is pretinned with soft solder.) The substrates are prepared for the evaporation of the film by cleaning them in a detergent solution, followed by immersion in hot (about 140°C) chromic acid cleaning solution. They are then rinsed in de-ionized water, pure acetone, and pure benzene, and stored until needed in a vapor degreaser which uses reagent-grade isopropyl alcohol. Before mounting the substrate in the cryostat, eight gold electrodes are deposited on it by vacuum evaporation. These provide four-terminal current and voltage leads for two simultaneously deposited bismuth films, which are produced side by side, on the same substrate. The bismuth-alloy films are $\frac{1}{8}$ in. wide, and the spacing between the voltage electrodes is $\frac{1}{2}$ in.

The alloy pellets used in the flash evaporation to make the film are cut with a lean knife from a 5-g ingot. The ingot is made by melting weighed amounts of bismuth and impurity in a clean Pyrex tube under high vacuum. After the material has been melted and outgassed, it is allowed to solidify, and the tube is sealed off from the vacuum system. The material is then remelted and thoroughly agitated to homogenize it. After the melt has been agitated for about 2 min, the tube is placed in a compressed-air stream, which solidifies the material in about 15 sec. The bismuth alloy is kept in the evacuated Pyrex capsule until needed. The bismuth, lead, and antimony were 99.999% pure, and were obtained from the American Smelting and Refining Company. The thallium was 99.99% pure, and was purchased from A. D. Mackay, Inc.

The alloy evaporation is performed by dropping a number of small pellets singly onto the filament. The pellets are placed in holes drilled radially into a brass drum, which rotates inside a closely fitting cover. As the drum is rotated, the pellets fall out of a hole in the bottom of the cover, through a tube, and onto the filament. The tube guides the pellets, and is bent to prevent bismuth from being deposited in the holes in the drum. The shaft which turns the drum passes through a double O-ring seal, and the space between the O-ring is evacuated when the shaft is turned. This minimizes any gas inflow during the shaft rotation. The pellets are about 5 mg in weight, and a total of 55 mg is used in each evaporation. Because the pellets land at different points on the filament and sometimes bounce off it, the thickness of the films vary somewhat.

The evaporation procedure is as follows. The filament is heated; the shutter is opened; the pellets are all dropped within 10 or 20 sec; the shutter is closed; and the current turned off. The substrate temperature

during the evaporation is 4.2°K. The pressure in the space outside the 77°K heat shield is about 5×10^{-7} Torr during the evaporation; the pressure around the substrate is undoubtedly lower, since that region is surrounded by surfaces at 4.2°K.

D. Measurement of the Critical Temperature and Thickness of the Film

The sample temperature is measured by means of a calibrated germanium resistor, using a four-terminal system and a potentiometer. The thermal emf in the resistor leads is measured and subtracted. Since the potentiometer can be read to $\pm 1 \mu\text{V}$, the random error in the temperature measurement is about ± 0.5 mdeg near 6°K. This is consistent with the scatter in a given run. From the observed constancy of the film resistance in the region where it changes rapidly, it can be concluded that the temperature fluctuates less than 0.1 mdeg during the taking of a reading. The critical temperatures are thought to be correct within 20 mdeg on an absolute scale, and correct relative to each other within 10 mdeg.

After making the film, the liquid helium in the inner tank is boiled off by means of a heater inserted down the pumping tube; the tank is then evacuated to reduce the heat capacity, and the temperature is regulated by manually controlling the current supplied to the heater attached to the copper block.

The determinations of the sample resistance at different temperatures are made with an alternating current generator, a lock-in amplifier, and a recorder. A 1000-cps signal, with an amplitude of 70 nA or less, is passed through the sample via the two end electrodes, and the resulting voltage generated across the middle electrodes is measured. The current is low enough so that there is no measurable dependence of sample resistance on current, even up to 10 times the current used in the final measurements.

After the film is deposited and the liquid helium is boiled off as previously described, the temperature is brought up slowly toward the critical temperature. When a sharp increase in film resistance indicates that the transition point has been reached, the temperature is further increased by a few hundredths of a degree, and the sample current and lock-in amplifier gain are adjusted to give a reading of nearly full scale on the recorder. The temperature is then reduced to about 20 or 30 mdeg below the midpoint of the transition. Then the temperature is raised in steps, and the resistance is measured at successively higher temperatures. About 25 points are taken on each curve, allowing 2 or 3 min between points to establish thermal equilibrium at the new temperature. After all the data have been taken, the temperature is raised about 0.3 to 0.5 deg, and another reading is recorded. The residual resistance is then measured at this temperature by passing direct current through the sample and measuring the

²⁵ N. V. Zavaritskii, Dokl. Akad. Nauk SSSR **86**, 687 (1952).

voltage drop across the middle electrodes with a potentiometer. The current is measured by the voltage drop across a calibrated resistor in series with the film. This calibrates the gain of the amplifier.

After the run is over, the sample is allowed to warm up to room temperature, keeping it always in high vacuum. Then the entire sample is covered with a thin film of silver, about 1000 Å thick. This film protects the bismuth-alloy film from oxidation after it is taken from the cryostat, and gives the whole surface of the sample a uniform and high reflectivity, which is necessary for the optical-interference method²⁴ used to measure the thickness.

III. RESULTS

A. Transition Widths and Critical Temperatures

Figure 2 shows the transition curve for sample e, containing 1.02 at.% thallium. The shape and width of the transition curve do not differ very much for different samples, with the exception of sample p. (The transition of this sample was about twice as wide as those of the other samples, for unknown reasons.) Note that after the film temperature has been raised about 0.3°K above the transition temperature, there is a small irreversible downward shift in the transition curve. On rewarming from below, the transition curve shows no change within the measurement error, i.e., there is no further measurable hysteresis. This behavior was seen in all of those samples in which further data were taken after measuring the residual resistance at a temperature substantially (0.3 to 0.5°K) above the critical temperature.

In the present investigation, the critical temperature is defined as the temperature at which the film has half of its normal-state resistance. Since small changes occur in the transition curve when the film is warmed 0.3 to 0.5°K above the transition temperature, the quoted critical temperatures are determined before that is done.

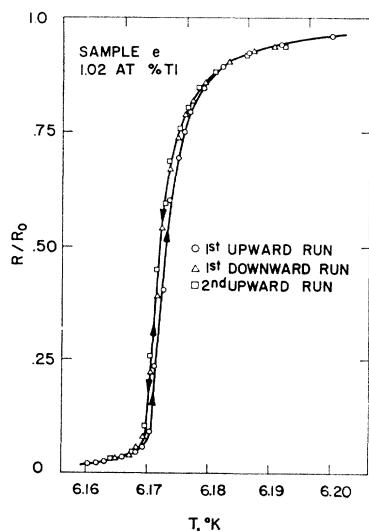


FIG. 2. Transition curve for sample e.

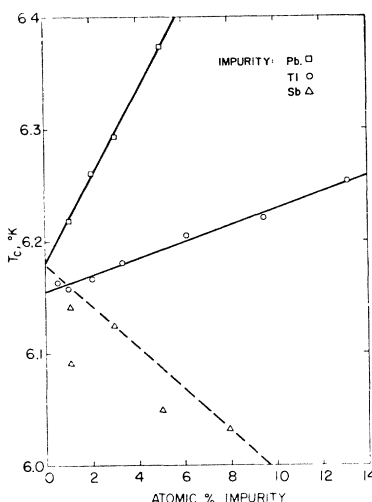


FIG. 3. Transition temperature versus impurity concentration for lead, thallium, and antimony impurities in amorphous bismuth.

It is found that the critical temperatures of the two simultaneously condensed sample films do not differ by more than 2 mdeg.

Figure 3 shows the observed transition temperatures as a function of impurity concentration. For the lead and thallium alloys, the data show an approximately linear dependence of the transition temperature on impurity content. For the antimony alloys, the data show a large amount of scatter, with the transition temperatures of the thinner samples lying lower than those of the thicker ones. This is especially clear for the two samples containing 1.08 at.% antimony, in which the thicker sample has a transition temperature about 50 mdeg higher than the thinner one. We cannot account for this. The film thicknesses are listed in Table I.

For the lead and thallium alloys, straight lines have been fitted by least squares. In the least-squares fitting,

TABLE I. Properties of the films.

Sample	At.% impurity	Thickness (Å)	Resistivity ($\mu\Omega$ cm)	T_c (°K)	Transition width (mdeg)
a	0	750±40	125±7	6.154	5.8
b	0 ^a	690±40	96±6	6.173	4.6
c	0.53 Tl	630±40	101±6	6.164	4.9
d	1.02 Tl	610±40	114±7	6.158	6.0
e	1.02 ^a Tl	6.173	4.5
f	2.05 Tl	550±40	97±7	6.167	5.7
g	3.32 Tl	820±40	134±7	6.181	5.6
h	6.15 Tl	6.205	6.0
i	9.52 Tl	550±40	114±8	6.220	5.6
j	13.16 Tl	730±40	114±8	6.253	...
k	1.03 Pb	920±40	144±6	6.218	5.2
l	2.02 Pb	740±40	129±7	6.261	6.3
m	3.08 Pb	750±40	130±7	6.292	5.3
n	5.09 Pb	700±40	118±7	6.374	6.2
o	1.08 Sb	890±20	141±3	6.142	5.1
p	1.08 Sb	480±20	141±6	6.092	9.5
q	2.95 Sb	1070±20	144±3	6.125	4.5
r	5.02 Sb	540±20	125±5	6.049	6.5
s	7.96 Sb	1130±20	138±2	6.032	5.0

^a Made with the substrate at 1.5°K.

the points for pure bismuth have not been used, since it was found that for pure-bismuth films the condensation temperature has a noticeable effect on the transition temperature. A pure bismuth film made at 1.5°K was found to have a transition temperature about 20 mdeg higher than one made at 4.2°K. Concerning films containing 1.02 at.% thallium, one made at 1.5°K had a transition temperature only 7 mdeg higher than one made at 4.2°K. This is to be expected, since impurities stabilize the amorphous state; they raise the temperature at which the film transforms into the semimetallic state; they raise the temperature at which the film transforms into the semimetallic state, in some cases nearly to room temperature.^{22,23}

For the antimony alloys, because of the apparent thickness effect, a straight line (shown dashed in Fig. 3) has been arbitrarily drawn through the points for the two thickest samples (both about 1100 Å thick), giving a slope in good agreement with the data of Barth.²²

In making the least-squares analysis, it has been assumed that all of the error is in the measurement of the transition temperatures. A partial confirmation of this assumption can be found from an inspection of the lead data. If all of the scatter in the lead data in Fig. 3 is assumed to be due to composition fluctuations, the mean deviation of the melt composition from the fitted line would be only 0.1 at.%. A chemical analysis of the thallium samples by flame absorption spectroscopy gave results in agreement with the melt composition of the starting material, but the accuracy of the chemical analysis was not better than ± 3 at.%.

For both the lead and thallium impurities, the root-mean-square deviation of the experimental points from the fitted line is about 4 mdeg. This scatter in the experimental data is probably due to small differences in the deposition rate, duration of the evaporation, film thickness, etc., which could not be held exactly the same from run to run. It was found that the two simultaneously deposited sample films had slightly different transition temperatures, the difference in no case exceeding 2 mdeg. This indicates that there is a small variation in the critical temperature, even under presumably identical deposition conditions.

It is evident from Fig. 3 that the least-squares-fitted straight lines do not all pass through the same point for pure bismuth. For the lead and thallium impurities, the difference between the extrapolated transition temperatures for pure bismuth is significantly greater than the sum of the mean deviations from the fitted lines (8 mdeg). The reason for this is not known. It seems that the curves for the transition temperature versus impurity concentration are slightly nonlinear for small concentrations. This nonlinearity is much less than that which results from the anisotropy effect, which is seen in crystalline superconductors.⁵

B. Resistivities

There is considerable scatter in the resistivities of the samples, as seen in Table I. We believe this does not result from inaccurate measurements of film thickness; the precision of these thickness measurements is too high to permit such an explanation. Possibly, irregularities in the film structure on a macroscopic scale are responsible for the scatter in the resistivities. At any rate, there does not seem to be any systematic shift of the resistivity with impurity concentration. This is not surprising, if amorphous bismuth is regarded as being in a kind of frozen liquid state. Experiments on liquid metal alloys show that the usual rules describing the resistance due to impurities in crystalline solids are not valid for liquid metals.²⁶ (In some cases the resistivity actually decreases when impurities are added to a pure liquid metal.) Because we can see no systematic variation of resistivity with impurity concentration in our samples, and because there is no apparent correlation between the scatter in the resistivity values and the scatter in the critical temperatures, we feel safe in setting $\alpha\delta\rho$ equal to zero in Eq. (1). Therefore, if the amorphous bismuth alloys have a valence effect with the same kind of behavior as that of crystalline tin and indium, we expect that

$$\delta T_c = \beta n^i \delta z. \quad (2)$$

IV. DISCUSSION

A. Critical Temperatures

In the previous section, we have seen that the valence effect δT_c for a given impurity concentration is expected to be proportional to δz if amorphous bismuth has a valence effect similar to that of crystalline tin and indium. Thallium, lead and bismuth occur together in the periodic table, in the stated order; antimony is located above bismuth. Hence, thallium should shift T_c twice as much as lead, and antimony should not shift it at all. The data shown in Fig. 3 show this is not true. The free-atom size of the impurity atoms also seems uncorrelated with δT_c . In short, there is no direct relationship between the gross properties of the impurity atoms and the δT_c which they cause.

This remarkable situation seems closely analogous to the breakdown of Linde's rule in liquid alloys.²⁶ The rule states that a small concentration of impurity atoms changes the electrical resistance of a material by an amount proportional to $(\delta z)^2$, the square of the valence difference between impurity atom and host metal. Apparently the resistivity of an amorphous material (like a liquid) is affected by something other than the gross properties of the impurity atoms.

Faber and Ziman have considered this situation from the theoretical side.²⁶ They suggest that the arrangement of the atoms in an amorphous substance accentuates

²⁶ T. E. Faber and J. M. Ziman, *Phil. Mag.* **11**, 153 (1965).

ates the influence of incoherent electron collisions with large momentum transfer. These collisions probe the detailed structure of the impurity atom's core. As a result, the influence of an impurity atom on the resistivity of an amorphous metal is not simply related to that atom's gross properties. Because resistivity and superconductivity both arise from the electron-lattice interaction, we suggest that the same general argument may explain why the impurity-induced shift in the superconducting critical temperature of amorphous bismuth has no simple relation with the impurity's valence or atomic size. A theoretical calculation should be carried out to test this idea.

B. Transition Widths and Coherence Lengths

It is convenient and customary to define the width W of the superconducting transition to be the difference between the temperatures where the sample resistance is 25 and 75% of the normal-state residual resistance. In our samples, W ranged from 4.5 to 6.5 mdeg, with the exception of one very thin sample (sample p), for which W was 9.5 mdeg.

The width of the superconducting transition has been accounted for by Pippard²⁷ in terms of the coherence length in the superconducting state. He assumed that it is impossible to have a superconducting region smaller than a certain critical size, approximately two coherence lengths $2\xi_P$ across. The energy fluctuations in such a region are computed, and the probability of finding it in the superconducting state at any temperature is calculated. By making assumptions about the size and shape of the superconducting regions, it is then possible to calculate the resistivity of the sample as a whole, as a function of temperature. The following equation is then obtained:

$$\xi_P = 1.07(k_B T_c^2 / \pi C_n W^2)^{1/3}, \quad (3)$$

where k_B is the Boltzmann constant, C_n is the normal-state specific heat per unit volume, and W is the width of the transition (as defined above).

To calculate the coherence length, it is necessary to know the normal-state specific heat. We have estimated the electronic specific heat from the free-electron model, and the lattice specific heat has been calculated using the Debye temperature ($\Theta_D \approx 100^\circ\text{K}$ at 6°K)²⁸ of semi-metallic bismuth. This is reasonable, since for some other elements (e.g., tin) the Debye temperatures of different allotropic forms are roughly equal, even though the electronic band structures may be quite different. With these assumptions, Eq. (3) indicates that the coherence length ξ_P in our samples is about 700 Å.

The coherence length enters Pippard's formula for the transition width as a phenomenological parameter. Consequently, this formula *defines* a coherence length, which may not be the same as that involved in other

superconducting phenomena. There are two lengths relating to a superconductor which are commonly referred to as "the coherence length."

One of these can be called the electromagnetic coherence length, which we denote by ξ_e .²⁹ It is a parameter in the integral relating current density \mathbf{J} to vector potential \mathbf{A} in a superconductor. The vector potential \mathbf{A} at a certain point affects the current density \mathbf{J} at all points within a distance of order ξ_e . The electromagnetic coherence length depends very little on temperature.³⁰

For a pure superconductor, the electromagnetic coherence length is given approximately by

$$\xi_e = \hbar v_F / \pi \Delta(0) \equiv \xi_0, \quad (4)$$

where v_F is the Fermi velocity and $\Delta(0)$ is the superconducting gap parameter at absolute zero.^{29,31}

For impure superconductors, ξ_e is given by

$$(1/\xi_e) = (1/\xi_0) + (1/\alpha l), \quad (5)$$

where l is the electron mean free path, and α is a dimensionless parameter of order unity.

At one time it was thought that ξ_e was approximately equal to the coherence length ξ_P in Eq. (3), which limits the sharpness of the superconducting transition. The transitions in our films are too sharp for this to be true. For our samples, Eq. (5) indicates that $\xi_e \approx 5 \text{ \AA}$, if we use the free-electron model to find l (with $m/m^* = 1$). The discrepancy between this value and the coherence length, $\xi_P = 700 \text{ \AA}$, calculated from the width of our transitions, provides perhaps the clearest experimental indication which has been seen, that ξ_e does not limit the width of the transition.

We believe that thermal fluctuations in a superconductor are limited by another coherence length, ξ_{LG} . This is called the "Landau-Ginzburg" coherence length, since it appears as a characteristic length in the Landau-Ginzburg theory. According to present theory, if there is a disturbance in a superconductor which affects the gap parameter Δ , this change in Δ will decay in distance, with a characteristic length ξ_{LG} . In a dirty superconductor, this is given by³²

$$\xi_{LG} = [\xi_0 l / (1 - T/T_c)]^{1/2}. \quad (6)$$

The theory of the resistive transition to the superconducting state in the presence of thermal fluctuations is undeveloped up to the present time, because of the great difficulty of the problem. We build on Pippard's ideas,²⁷ using a coherence length ξ_R , closely related to ξ_{LG} , to make a crude and speculative estimate of the

²⁹ A. B. Pippard, Proc. Roy. Soc. (London) **A216**, 547 (1953).

³⁰ J. R. Waldram, Rev. Mod. Phys. **36**, 187 (1964).

³¹ J. Bardeen and J. R. Schrieffer, in *Progress in Low Temperature Physics*, edited by C. J. Gorter (North-Holland Publishing Company, Amsterdam, 1961), Vol. III.

³² C. Caroli, Physik. Kondensierten Materie **3**, 345 (1965).

²⁷ A. B. Pippard, Proc. Roy. Soc. (London) **A203**, 210 (1950).

²⁸ P. H. Keesom and N. Pearlman, Phys. Rev. **96**, 897 (1954).

ideal width of the resistive transition, by making the following assumptions:

1. The width of the resistive transition is finite, because at a given temperature T , spherical regions of size $4\pi\xi_R^3/3$ fluctuate into the superconducting state.

2. For $T > T_c$, ξ_R is given by

$$\xi_R = [\xi_0 l / |1 - T/T_c|]^{1/2}. \quad (7)$$

It should be noted that the temperature dependence of ξ_R is plausible, because of Eq. (6), but that the Landau-Ginzburg theory is valid only for $T < T_c$. Equation (7) is therefore only a rough estimate.

3. The fluctuations described above occur slowly enough so the current density can adjust to them easily.

4. Each superconducting region has zero resistance, and there is negligible electron scattering at the boundary of each region.

Using these assumptions, we repeat Pippard's treatment, but with our temperature-dependent coherence length ξ_R . We find, using the notation of Doidge,³³ that the resistance R is related to the normal-state resistance R_n by the equation

$$\frac{R}{R_n} = \frac{1 - (1/\sqrt{\pi})E(\gamma\tau)}{1 + (2/\sqrt{\pi})E(\gamma\tau)}, \quad (8)$$

where

$$E(x) = \int_x^\infty e^{-y^2} dy, \quad (9)$$

$$\gamma = [(4/3)\pi\xi_R^3 C / 2kT_c^2]^{1/2}, \quad (10)$$

$$\tau = T - T_c, \quad (11)$$

k is Boltzmann's constant, and C is the specific heat per unit volume. We then calculate that R/R_n should increase from $\frac{1}{4}$ to $\frac{3}{4}$ in a temperature interval W given by

$$W = [0.15T_c / (\xi_0 l)^2] (k/C)^2. \quad (12)$$

We estimate C as described above in the paragraph following Eq. (3), and compute ξ_0 from Eq. (4) by using the free-electron model with five electrons per atom³⁴ to obtain v_F . We then obtain $W = 8 \times 10^{-8}$ °K. Since this is so much less than the observed width of the transition, $\sim 5 \times 10^{-3}$ °K, we feel that thermal fluctuations do not limit the narrowness of the transitions in our films. Presumably, strains and inhomogeneities are responsible for the observed transition width. Since our samples have transitions among the sharpest ever observed in films, we feel they are of relatively high quality.

It should be emphasized that our rough calculation of W is speculative. In a pure superconductor, where ξ_{LG}

is given by

$$\xi_{LG} = \xi_0 / [1 - T/T_c]^{1/2}, \quad (13)$$

Eq. (12) would be replaced by

$$W = (0.15T_c / \xi_0^6) (k/C)^2. \quad (14)$$

It is interesting that this expression indicates that W/T_c would be proportional to $(T_c/\mu)^4$, where μ is the chemical potential, if we were to ignore the lattice specific heat. This same factor occurs in the calculation³⁵ which has been done to find the width of the transition which would be observed in a measurement of specific heat. That calculation used thermal Green's functions; it was done only for a pure superconductor, with the lattice specific heat left out.

ACKNOWLEDGMENTS

It is a pleasure to acknowledge helpful comments by B. D. Josephson and L. P. Kadanoff.

APPENDIX

There have been several measurements of physical constants of amorphous bismuth. Others can be

TABLE II. Properties of amorphous bismuth.

<i>Experimental Properties</i>	
1. Resistivity	$\sim 100 \mu\Omega \text{ cm}$
2. Transition temperature	$6.17 \pm 0.03^\circ \text{K}$
3. Energy gap (2Δ) ^a	2.15 meV
4. Reduced gap ($2\Delta/kT_c$)	4.1
5. Hall coefficient ^b	$-2.9 \times 10^{-6} \text{ cm}^3/\text{C}$
6. Heat of transformation ^c	1.5 kcal/mole
<i>Free-Electron Model</i>	
7. Electron density (5 el./atom, 9.8 g/cc)	$1.4 \times 10^{23} \text{ cm}^{-3}$
8. Fermi velocity ($m^*/m = 1$)	$1.9 \times 10^8 \text{ cm/sec}$
9. Mean free time ($\sigma m/Ne^2$)	$2.5 \times 10^{-16} \text{ sec}$
10. Reciprocal mean free time (in energy units)	2.6 eV
11. Mean free path	4.7 Å
12. Fermi energy ($m^*/m = 1$)	9.8 eV
13. Electronic-specific-heat coefficient ($5\pi^2 R/2T_f$)	$1.8 \times 10^4 \text{ erg/mole } ^\circ \text{K}$
14. Hall coefficient	$-4.5 \times 10^{-5} \text{ cm}^3/\text{C}$
<i>Superconductivity Theory</i>	
15. $\xi_0 \equiv (\hbar v_f / \pi \Delta)$	3600 Å
16. Electromagnetic coherence length $\xi_c \cong (\xi_0^{-1} + l^{-1})^{-1}$	4.7 Å
17. London penetration depth $(m/Ne^2\mu_0)^{1/2}$	140 Å
18. Thermodynamic critical field $(5.88\gamma T_c^2)^{1/2}$	430 Oe

^a F. Reif and M. Woolf, Phys. Rev. Letters 9, 315 (1962).

^b W. Buckel, Z. Physik 154, 474 (1959).

^c W. Sander Z. Physik 147, 361 (1957).

estimated from theoretical models. Table II lists the constants which have been most useful to us in our work.

³³ P. R. Doidge, Phil. Trans. Roy. Soc. London A248, 553 (1956).

³⁴ W. Buckel, Z. Physik 154, 474 (1959).

³⁵ E. G. Batyev, A. Z. Patashinskii, and V. L. Pokrovskii, Zh. Eksperim. i. Teor. Fiz. 46, 2093 (1965) [English transl.: Soviet Phys.—JETP 19, 1412 (1964)].